Zewail City of Science and Technology

Numerical Solution of the 2D Incompressible Navier–Stokes Equations

Lid-Driven Cavity Flow Using a Fractional Step Method

Course: Partial Differential Equations

Instructor: Dr. Abdallah Awad

Submitted by:

Abdelrahman Taha (202300062)

Ahmed Essam (202301992)

December 30, 2025

Contents

1 Introduction

The lid-driven cavity flow is a classical benchmark problem for incompressible flow solvers. Despite its simple geometry, it exhibits rich flow physics, including strong vortical structures and secondary corner vortices at moderate and high Reynolds numbers. Because of the availability of high-quality benchmark solutions, most notably those of Ghia et al. (1982), this problem is widely used to validate numerical schemes for the incompressible Navier–Stokes equations.

In this work, the two-dimensional incompressible Navier–Stokes equations are solved using a fractional step (projection) method on a staggered grid. The pressure Poisson equation is solved using a discrete cosine transform (DCT), which provides an efficient direct solver on a rectangular domain.

2 Governing Equations

2.1 Incompressible Navier–Stokes Equations

The incompressible Navier–Stokes equations in non-dimensional form are

$$\frac{\partial \mathbf{u}}{\partial t} + (\mathbf{u} \cdot \nabla)\mathbf{u} = -\nabla p + \frac{1}{Re}\nabla^2 \mathbf{u}, \tag{1}$$

$$\nabla \cdot \mathbf{u} = 0, \tag{2}$$

where $\mathbf{u} = (u, v)$ is the velocity vector, p is the pressure, and Re is the Reynolds number.

2.2 Meaning of the Reynolds Number

The Reynolds number compares inertial (convective) transport to viscous diffusion:

$$Re = \frac{UL}{\nu}, \tag{3}$$

where U is a characteristic velocity (the lid speed), L is a characteristic length (cavity size), and ν is the kinematic viscosity. Increasing Re corresponds to decreasing viscous effects, leading to thinner boundary layers near walls and stronger vortical motion.

2.3 Role of Pressure in Incompressible Flow

For incompressible flow, pressure does not have a separate evolution equation. Instead, pressure acts to enforce the kinematic constraint $\nabla \cdot \mathbf{u} = 0$. In numerical methods, this enforcement appears through the solution of a Poisson equation for pressure (or pressure correction) derived directly from the incompressibility condition. It acts as a Lagrange multiplier.

3 Numerical Method (Theory and Discretization)

3.1 Staggered (MAC) Grid and Variable Locations

A Marker-and-Cell (MAC) staggered grid is employed:

- Pressure $p_{i,j}$ is stored at cell centers.
- Horizontal velocity $u_{i+\frac{1}{2},j}$ is stored at vertical faces.
- Vertical velocity $v_{i,j+\frac{1}{2}}$ is stored at horizontal faces.

This arrangement improves the discrete coupling between pressure and velocity and helps avoid spurious pressure oscillations (often called checkerboard modes).

Let

$$\Delta x = \frac{L_x}{N_x}, \qquad \Delta y = \frac{L_y}{N_y}. \tag{4}$$

3.2 Conservative Form of the Convective Terms

The nonlinear convective term $(\mathbf{u} \cdot \nabla)\mathbf{u}$ can be written in conservative form (for incompressible flow) as the divergence of fluxes:

$$(\mathbf{u} \cdot \nabla)u = \frac{\partial(u^2)}{\partial x} + \frac{\partial(uv)}{\partial y}, \tag{5}$$

$$(\mathbf{u} \cdot \nabla)v = \frac{\partial(uv)}{\partial x} + \frac{\partial(v^2)}{\partial y}. \tag{6}$$

This form is convenient on a staggered grid because u and v represent face fluxes naturally.

3.3 Diffusion Term (Laplacian)

The viscous diffusion is given by:

$$\nabla^2 u = \frac{\partial^2 u}{\partial x^2} + \frac{\partial^2 u}{\partial y^2}, \qquad \nabla^2 v = \frac{\partial^2 v}{\partial x^2} + \frac{\partial^2 v}{\partial y^2}, \tag{7}$$

and is discretized with second-order central differences.

3.4 Time Integration and Stability Considerations

A first-order explicit Euler time discretization is used:

$$\mathbf{u}^{n+1} = \mathbf{u}^n + \Delta t\, \mathcal{R}(\mathbf{u}^n, p^{n+1}), \tag{8}$$

where $\mathcal{R}$ represents the spatially discretized right-hand-side terms. For explicit schemes, Δt must satisfy stability restrictions from both advection and diffusion (e.g., CFL-type conditions). In practice, Δt is chosen conservatively to ensure stable convergence to steady state.

3.5 Fractional Step (Projection) Method: Step-by-Step Derivation

The core difficulty is enforcing both momentum conservation and the constraint $\nabla \cdot \mathbf{u} = 0$. The projection method splits the update into a pressure-free predictor step and a projection (correction) step.

Step 1: Compute intermediate velocity (predictor)

Compute an intermediate velocity (u^*, v^*) without the pressure term:

$$u^* = u^n + \Delta t \left[-\left(\frac{\partial (u^2)}{\partial x} + \frac{\partial (uv)}{\partial y} \right)^n + \frac{1}{Re} \left(\nabla^2 u \right)^n \right], \tag{9}$$

$$v^* = v^n + \Delta t \left[-\left(\frac{\partial (uv)}{\partial x} + \frac{\partial (v^2)}{\partial y} \right)^n + \frac{1}{Re} \left(\nabla^2 v \right)^n \right]. \tag{10}$$

The field (u^*, v^*) generally does not satisfy $\nabla \cdot \mathbf{u} = 0$.

Step 2: Pressure Poisson equation (enforce incompressibility)

Define the corrected velocity:

$$\mathbf{u}^{n+1} = \mathbf{u}^* - \Delta t \nabla p^{n+1}. \tag{11}$$

Taking divergence and enforcing $\nabla \cdot \mathbf{u}^{n+1} = 0$ yields:

$$\nabla^2 p^{n+1} = \frac{1}{\Delta t} \nabla \cdot \mathbf{u}^*. \tag{12}$$

On a MAC grid, the discrete divergence at cell centers is:

$$(\nabla \cdot \mathbf{u}^*)_{i,j} \approx \frac{u^*_{i+\frac{1}{2},j} - u^*_{i-\frac{1}{2},j}}{\Delta x} + \frac{v^*_{i,j+\frac{1}{2}} - v^*_{i,j-\frac{1}{2}}}{\Delta y}. \tag{13}$$

Step 3: Velocity correction (projection)

After solving (12), velocities are corrected using pressure gradients evaluated at faces:

$$u^{n+1}_{i+\frac{1}{2},j} = u^*_{i+\frac{1}{2},j} - \Delta t \, \frac{p^{n+1}_{i+1,j} - p^{n+1}_{i,j}}{\Delta x}, \tag{14}$$

$$v^{n+1}_{i,j+\frac{1}{2}} = v^*_{i,j+\frac{1}{2}} - \Delta t \, \frac{p^{n+1}_{i,j+1} - p^{n+1}_{i,j}}{\Delta y}. \tag{15}$$

This step enforces $\nabla \cdot \mathbf{u}^{n+1} \approx 0$ up to discretization and solver accuracy.

3.6 Pressure Poisson Solver (DCT) and Solvability

The Poisson equation (12) is solved using a two-dimensional DCT, which is efficient for rectangular domains. Since pressure is defined up to a constant, the Poisson operator has a null space

corresponding to constant pressure. Numerically, this is handled by fixing the mean pressure (equivalently, setting the zero-frequency DCT mode to zero). In addition, for a Neumann-type Poisson problem, the right-hand side must satisfy a compatibility condition:

$$\int_{\Omega} (\nabla \cdot \mathbf{u}^*) \, d\Omega = 0, \tag{16}$$

which is typically enforced by subtracting the mean of the discrete right-hand side.

3.7 Stopping Criterion

Iterations continue until the steady-state change is sufficiently small:

$$\max\left(\|u^{n+1} - u^n\|_\infty, \ \|v^{n+1} - v^n\|_\infty\right) < \text{tol}. \tag{17}$$

4 Simulation Setup

4.1 Domain and Grid

The computational domain is a unit square with $L_x = L_y = 1$, discretized using $N_x = N_y = 128$ control volumes. The MAC staggering stores pressure at cell centers and velocities on cell faces.

4.2 Reynolds Numbers

Simulations are performed for:

$$Re = 400, \quad 1000, \quad 3200.$$

4.3 Lid Motion and Boundary Conditions

The flow is driven by the motion of the top boundary (the "lid") at $y = 1$. In the standard benchmark, the lid translates in the positive x-direction with constant non-dimensional speed $U_{\text{lid}} = 1$. The boundary conditions are:

$$u(x, 1) = 1, \qquad v(x, 1) = 0, \tag{18}$$

$$u(x, 0) = 0, \qquad v(x, 0) = 0, \tag{19}$$

$$u(0, y) = 0, \qquad v(0, y) = 0, \tag{20}$$

$$u(1, y) = 0, \qquad v(1, y) = 0. \tag{21}$$

The discontinuity at the top corners introduces strong shear. As Re increases, viscous diffusion weakens, boundary layers become thinner, and secondary corner vortices become more pronounced.

5 Results and Flow Interpretation

Figure 1 shows filled contours of the velocity magnitude $|\mathbf{u}| = \sqrt{u^2 + v^2}$. The largest velocities occur near the moving lid and near the right wall where the flow turns downward. As Re increases, the high-speed region becomes more confined to thin layers near boundaries and the interior circulation becomes stronger.

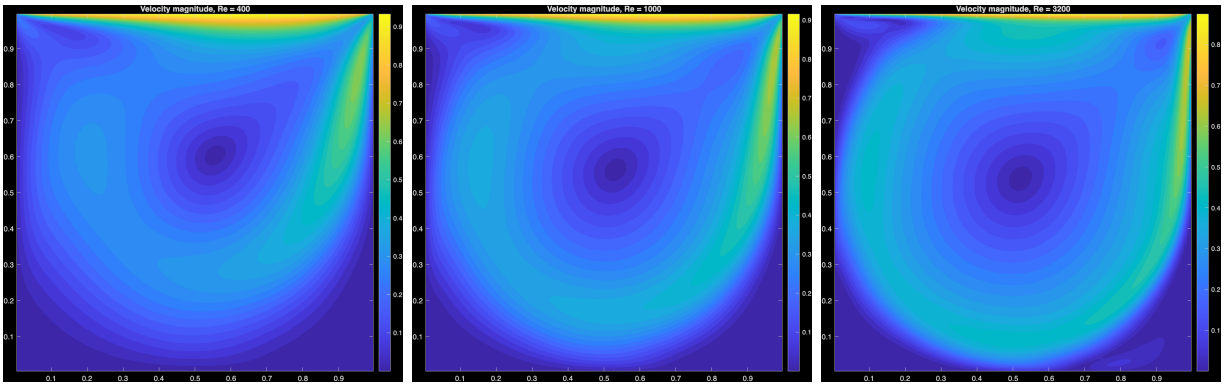

(a) $Re = 400$ (b) $Re = 1000$ (c) $Re = 3200$

Figure 1: Velocity magnitude contours for the lid-driven cavity at different Re.

6 Validation Against Ghia et al.

To validate the solver, velocities are compared against the benchmark data of Ghia et al. (1982) along cavity centerlines. Following their tables, we compare the point value $u(0.5, 0.9766)$ (Table I) and the point value $v(0.9688, 0.5)$ (Table II). We also report the maximum positive vertical velocity along the horizontal centerline $y = 0.5$.

Table 1: Centerline velocity comparison with Ghia et al. (1982).

	$u(0.5, 0.9766)$		$v(0.9688, 0.5)$		$\max_x v(x, 0.5)$ (positive)	
Re	This Work	Ghia	This Work	Ghia	This Work	Ghia
400	0.76120	0.75837	-0.14704	-0.12146	0.30217	0.30203
1000	0.66352	0.65928	-0.26850	-0.21388	0.37108	0.37095
3200	0.52142	0.53236	-0.49629	-0.39017	0.41688	0.42768

The agreement is very good for $u(0.5, 0.9766)$ and for the maximum positive value of v along $y = 0.5$. The discrepancy in $v(0.9688, 0.5)$ increases with Re, which is expected because near-wall gradients become sharper at higher Re and are more sensitive to grid resolution and time-stepping choices.

7 Conclusion

A two-dimensional lid-driven cavity flow was simulated using a fractional step method on a MAC staggered grid. Pressure was computed from a Poisson equation so that the velocity field satisfies incompressibility. The DCT-based Poisson solver provides an efficient approach on rectangular domains. The computed centerline quantities show good agreement with the benchmark results of Ghia et al. (1982), and the expected Reynolds-number dependence of boundary layers and vortical structures is observed.

References

[1] Ghia, U., Ghia, K., & Shin, C. (1982). High-Re solutions for incompressible flow using the Navier–Stokes equations and a multigrid method. *Journal of Computational Physics, 48*(3), 387–411. https://doi.org/10.1016/0021-9991(82)90058-4

[2] MathWorks.(2020). GitHub *mathworks/2D-Lid-Driven-Cavity-Flow-Incompressible-Navier-Stokes-Solver:* GitHub https://github.com/mathworks/2D-Lid-Driven-Cavity-Flow-Incompressible-Navier-Stokes-Solver

[3] Perot, J. (1993). An analysis of the fractional step method. *Journal of Computational Physics, 108*(1), 51–58. https://doi.org/10.1006/jcph.1993.1162